

# Jet Sweepback in the PWN of PSR J1709-4429

Martijn de Vries<sup>1</sup>, Roger Romani<sup>1</sup>, Oleg Kargaltsev<sup>2</sup>,  
George Pavlov<sup>3</sup>, Bettina Posselt<sup>3,4</sup> and Patrick Slane<sup>5</sup>

<sup>1</sup>Dept. of Physics and Kavli Institute for Particle Astrophysics and Cosmology, Stanford University, Stanford, CA 94305, USA

<sup>2</sup>Department of Physics, George Washington University, Washington, DC 20052, USA

<sup>3</sup>Department of Astronomy & Astrophysics, Pennsylvania State University, University Park, PA 16802, USA,

<sup>4</sup>Department of Physics, University of Oxford, OX1 3PU Oxford, UK

<sup>5</sup>Harvard-Smithsonian Center for Astrophysics, 60 Garden Street, Cambridge, MA 02138, USA



Contact: mndvries@stanford.edu

## Introduction

*Chandra* observations of PSR J1709-4429 and its associated pulsar wind nebula (PWN) reveal a distinct toroidal structure, equatorial outflow, and narrow polar jets. The jets are of particular interest, as they are swept back at scales of 2' by the pulsar motion. We present here preliminary results of new sensitive observations of J1709 totaling >650ks. With these new data we aim to

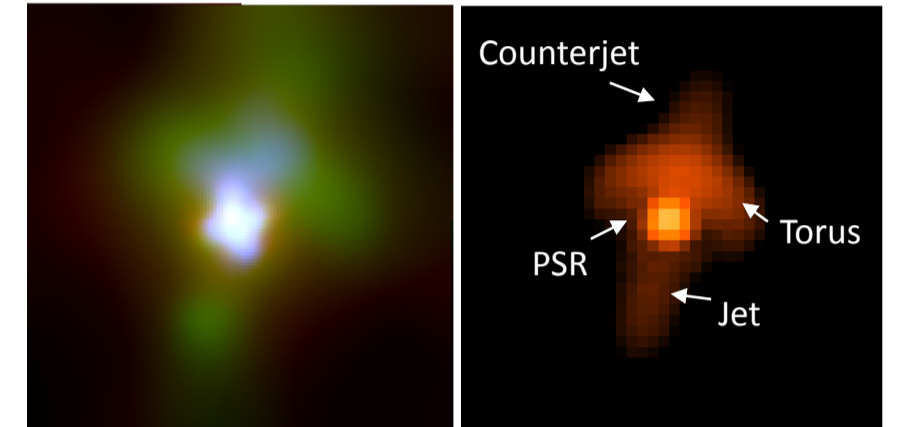
- 1) Constrain the jet perpendicular motion by comparing data from different epochs (10<sup>7</sup> s timescales)
- 2) Perform a sensitive spectral analysis of the torus, equatorial outflow, jets, and bow shock, probing the interaction between the PWN and the surrounding ISM
- 3) Determine or constrain the proper motion of the pulsar by comparing with archival data from 2000 and 2004. This will allow us to check the relationship with the nearby supernova remnant (SNR) G343.1-2.3, seen at radio wavelengths

Thus, with this study we can address a wide range of PSR/PWN/jet physics.

## Pulsar and torus

Maps of the core at subpixel resolution reveal the structure of the pulsar, torus, jet and counterjet. Romani et al. (2004) have previously fit the torus model and obtained values for the positional parameters, as well as the torus radial flow velocity ( $\beta = 0.70$ ).

**Figure 1** Left: 12.5"x12.5" RGB image of the torus, pulsar and outflow at *Chandra* subpixel resolution (1/5th of the normal pixel size), adaptively smoothed with *csmooth*. Red: 0.7 - 1.5 keV. Green: 1.5 - 3 keV. Blue: 3 - 8 keV. Right: model of the pulsar, torus, and jets (Romani et al., 2004)



## Large-scale X-ray and radio emission

Radio observations of SNR G343.1-2.3 reveal a spur of emission extending towards the location of the pulsar. Our deep *Chandra* exposures also show faint and diffuse emission along this radio spur, suggesting a connection between the two (Figure 2). Additionally, The HESS galactic plane survey shows TeV emission extending towards the pulsar.

Closer to the pulsar, we observe an equatorial outflow at radii of up to 25", and the X-ray jets seem to have punched a hole through the radio plasma (Figure 3).

We have performed a spectral analysis of several components in the system (Table 1). The photon index increases between the torus and the outflow, as the spectrum gets softer due to synchrotron losses.

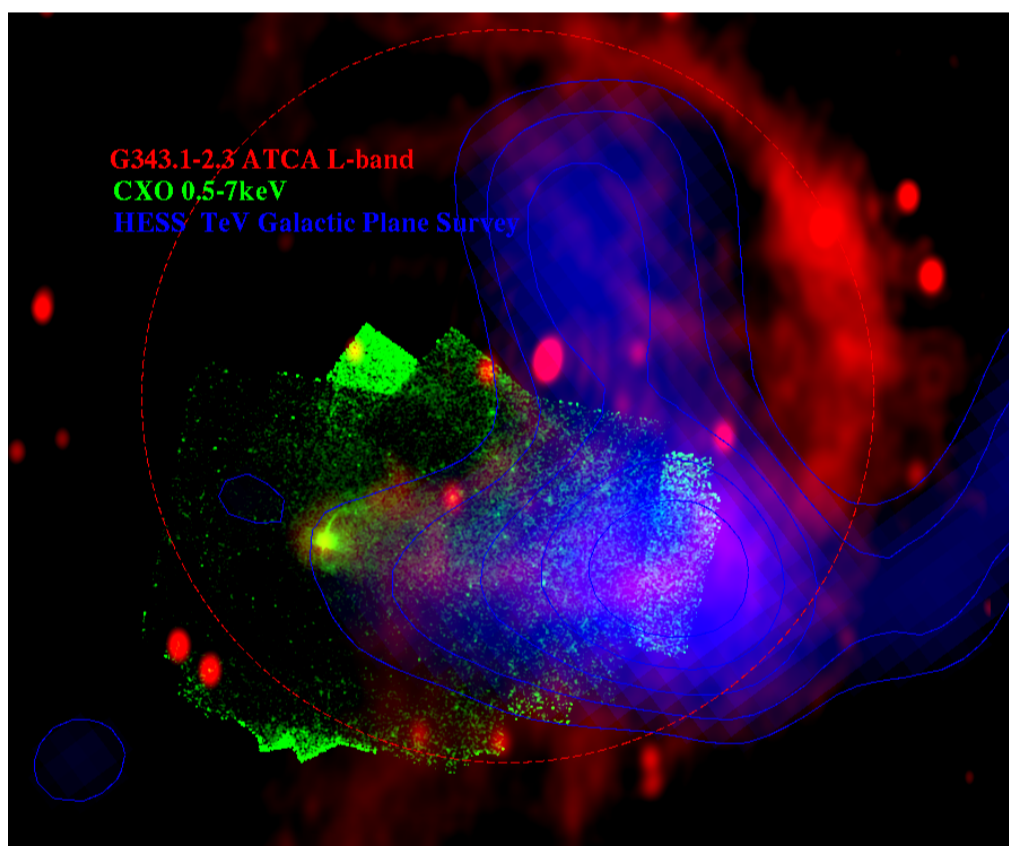


**Figure 2:** Composite color image of J1709-4429 and the nearby SNR. Green: *Chandra* ACIS exposure-corrected 0.5-7 keV mosaic of all observations, smoothed. Blue: HESS TeV Galactic Plane Survey contours and emission. Red: ATCA L-band (1.4 GHz) mosaic of SNR G343.1-2.3. The circle with radius 21.5' indicates the rim of the SNR

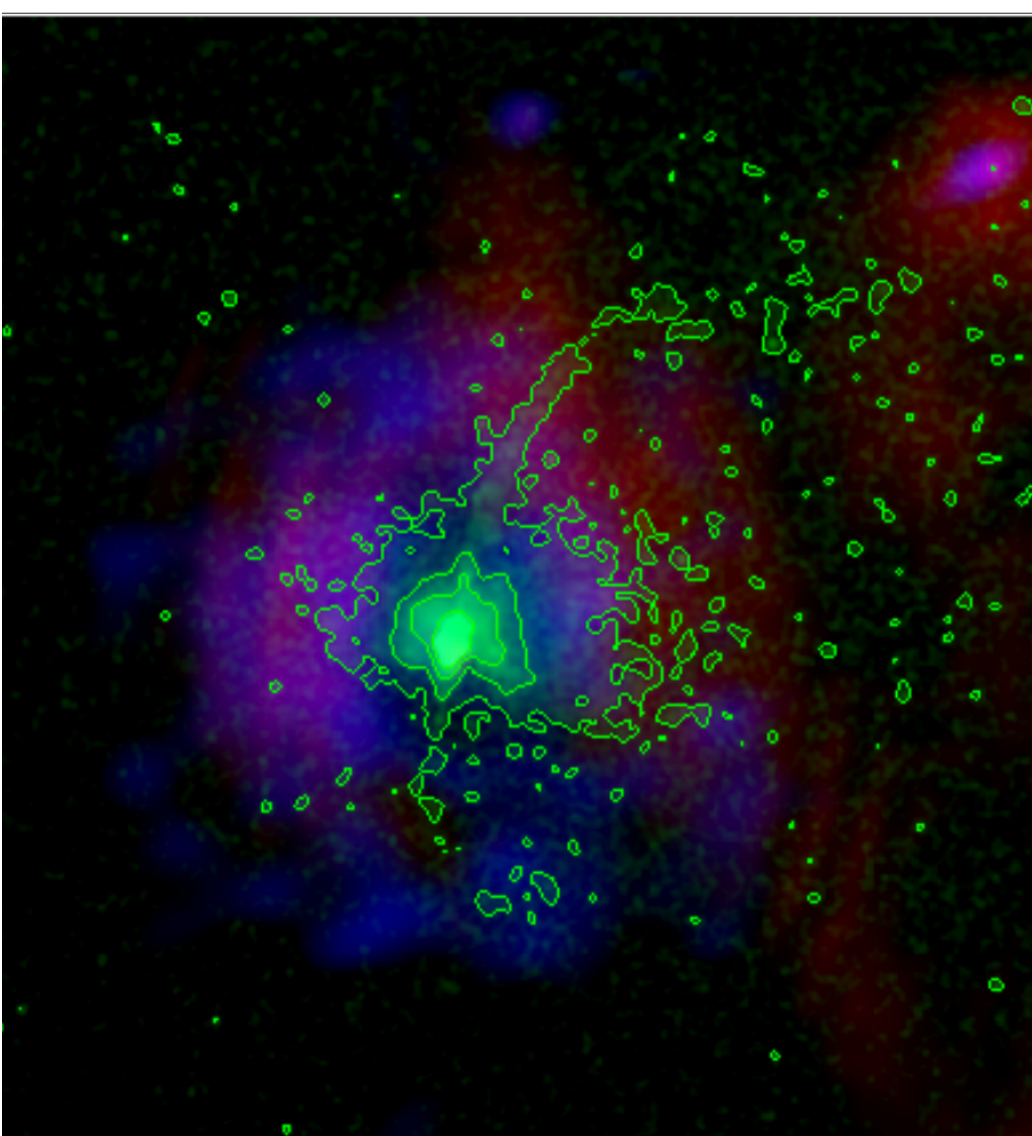


**Figure 3:** 6'x6' composite color image of the pulsar, outflow, and jets. Red: ATCA L-band (1.4 GHz). Green: *Chandra* ACIS exposure-corrected 0.5-7 keV image, smoothed by 2.5". Blue: ATCA C-band (4.8 GHz).

Structure	Model	$\Gamma / kT$ [keV]	$\chi^2/\text{dof}$
Pulsar	PL	$1.48 \pm 0.08$	244/258
	+ BB	$0.18 \pm 0.01$	
Torus	PL	$1.58 \pm 0.04$	225/223
Eq. Outflow	PL	$1.71 \pm 0.07$	431/436
Counterjet	PL	$1.50 \pm 0.07$	176/191
Outer C.-jet	PL	$1.48 \pm 0.23$	324/320
Jet	PL	$1.56 \pm 0.08$	321/338
Outer Jet	PL	$1.82 \pm 0.55$	255/252

**Table 1:** Results of spectral fits to several components in the system. Galactic absorbing column density was fixed to  $6 \times 10^{21} \text{ cm}^{-2}$  for all fits

## The Dynamic Jets

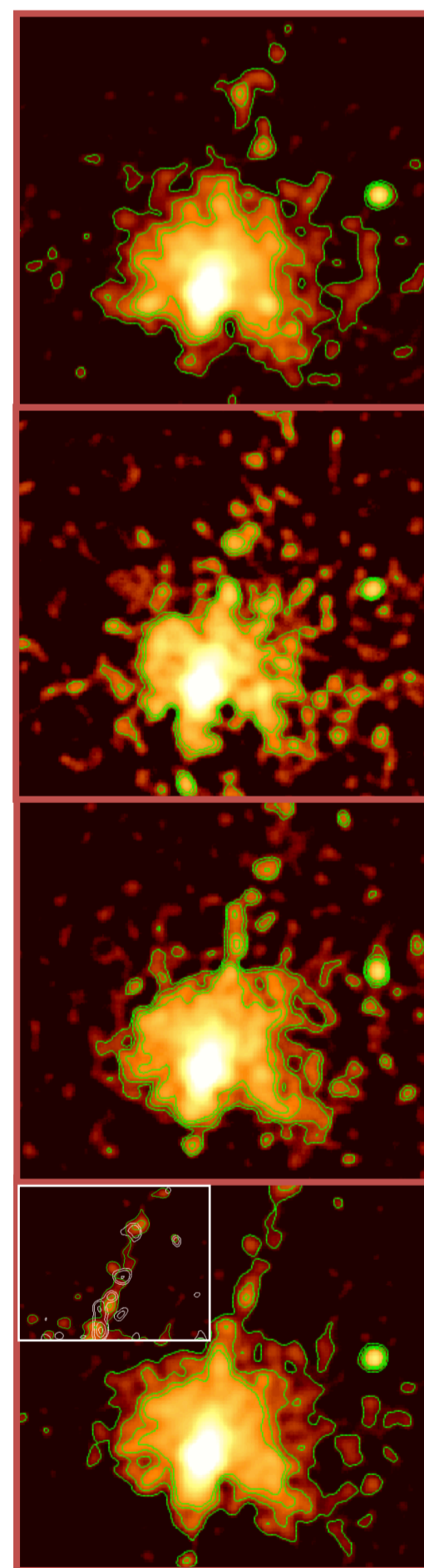


**Figure 4:** Exposure-corrected 1.5-8 keV *Chandra* ACIS image of the jets at different epochs. From top to bottom: Jun 2018 (230 ks), Oct 2018 (53 ks), Jan-Feb 2019 (173 ks), Jun-Jul 2019 (164 ks). Bottom panel, top left corner: The final epoch with green contours, with the contours of the previous epoch overlaid in white.

Figure 4 compares *Chandra* images of the pulsar jets at different epochs. This comparison reveals jet variability on timescales of months, similar to the Vela pulsar jet (Pavlov et al., 2003). The jets appear to show curved structure, as well as blobs appearing and disappearing between epochs. We also noticed two bright spots east and west of the pulsar in the first epoch, which will be investigated at a later time.

We analyzed the intra-epoch jet variability by using a cross-correlation routine to compare counts profiles of different epochs along the jet axis (Figure 5). Unfortunately, the data are noisy and we have not yet determined the statistical significance of the correlation. The fact that we obtain significantly different velocities for the jet and counterjet is hard to explain. These plots should therefore be interpreted as suggestive rather than conclusive.

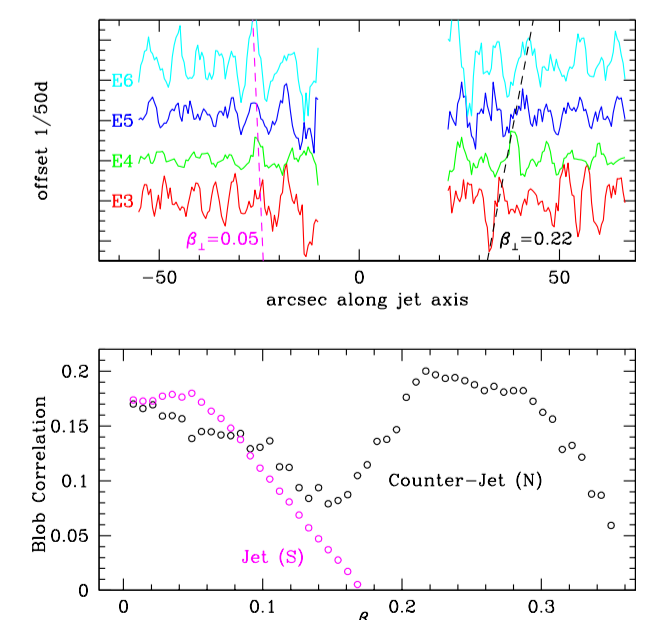


**Figure 5** Top: Counts profiles of the jet (towards the left) and counterjet (towards the right) at the epochs shown in Figure 4. The cross-correlation suggests blob motion of  $\beta_{\perp} = 0.05$  for the jet and  $\beta_{\perp} = 0.22$  for the counterjet Bottom: The result of the cross-correlation plot for both jets.